

# Bayesian Inference and Global Sensitivity Analysis for Ambient Solar Wind Prediction<sup>1</sup>

Opal Issan<sup>1,2</sup>    Pete Riley<sup>3</sup>    Enrico Camporeale<sup>4,5</sup>    Boris Kramer<sup>1</sup>

September 23rd, 2025

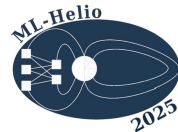
<sup>1</sup>University of California San Diego, USA

<sup>2</sup>Los Alamos National Laboratory, USA

<sup>3</sup>Predictive Science Inc., USA

<sup>4</sup>Queen Mary University of London, UK

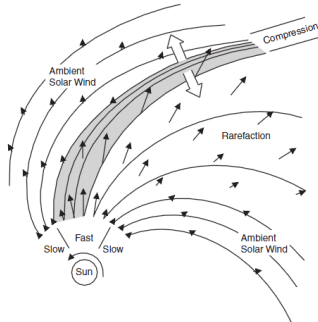
<sup>5</sup>University of Colorado, Boulder, USA



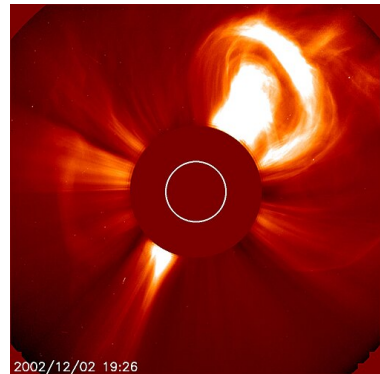
<sup>1</sup>This research was partially supported by the National Science Foundation (NSF) under Award 2028125.

# What is the ambient solar wind?

- The **ambient solar wind** is the long-lived, large-scale structure in the solar wind.
- **Corotating interaction regions** (CIR), regions between fast and slow solar wind, are the main driver of geomagnetic activity during **solar minimum**.
- **Coronal mass ejections** (CME) are modeled as perturbations to the ambient solar wind and are the main driver of geomagnetic activity during **solar maximum**.



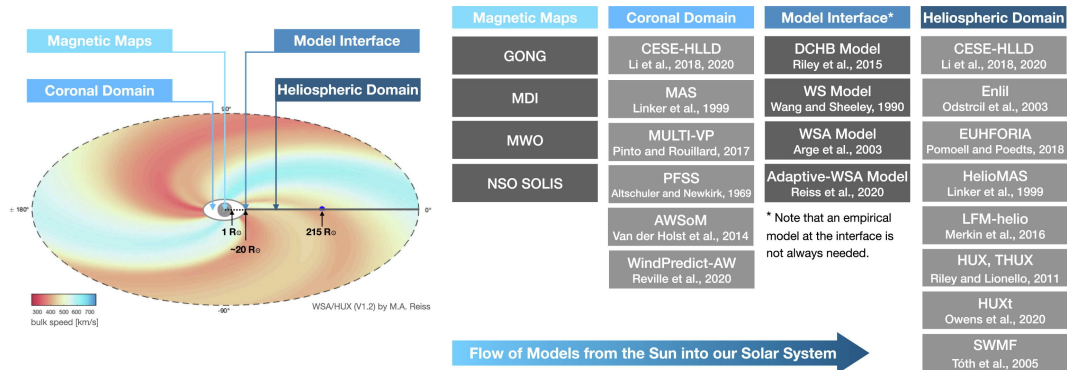
Schematic illustration of CIRs. Credit: [Pizzo, 1978]



CME in white-light coronagraph imagery. Credit: [Webb and Howard, 2012]

# State-of-the-art ambient solar wind models

State-of-the-art models for forecasting the ambient solar wind near Earth couple **coronal** and **heliospheric** models. NASA's CCMC available models<sup>2</sup>:

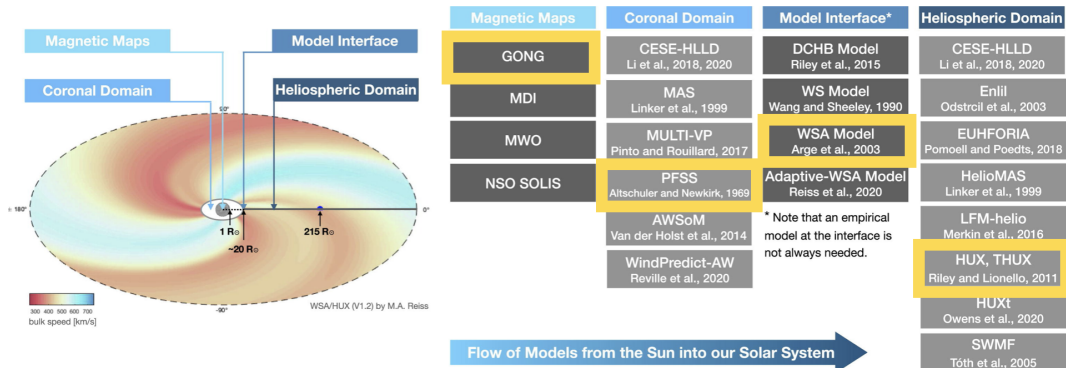


Credit: [Reiss et al., 2022]

<sup>2</sup><https://ccmc.gsfc.nasa.gov>

# State-of-the-art ambient solar wind models

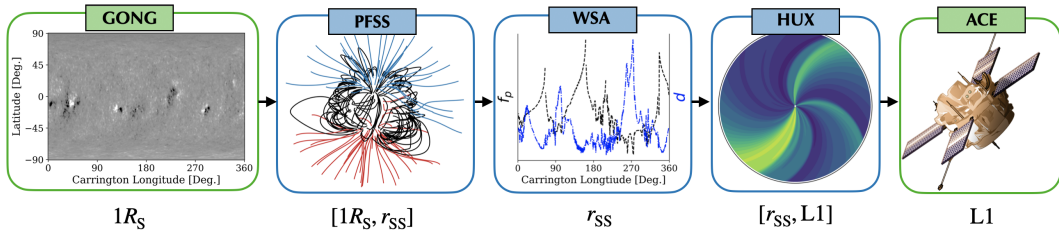
State-of-the-art models for forecasting the ambient solar wind near Earth couple **coronal** and **heliospheric** models. NASA's CCMC available models<sup>3</sup>:



Credit: [Reiss et al., 2022]

<sup>3</sup><https://ccmc.gsfc.nasa.gov>

# Highly efficient ambient solar wind model chain



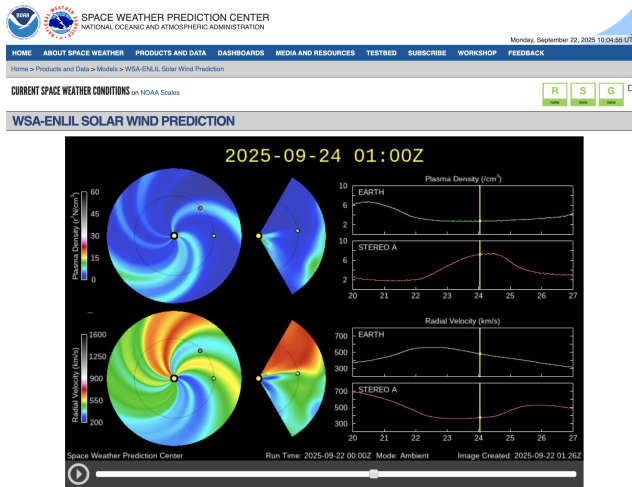
## Reduced-physics and semi-empirical models

- Potential Field Source Surface (**PFSS**) [Altschuler and Newkirk, 1969]  
 $\Rightarrow \nabla^2 \Psi = 0$
- Wang-Sheeley-Arge (**WSA**) [Arge et al., 2004]  $\Rightarrow$   
$$v_{wsa}(f_p, d) = v_0 + \frac{v_1 - v_0}{(1+f_p)^\alpha} \left( \beta - \gamma \exp \left( - \left( \frac{d}{w} \right)^\delta \right) \right)^\psi$$
- Heliospheric Upwind eXtrapolation (**HUX**) [Riley and Lionello, 2011]  $\Rightarrow$   
$$-\Omega_{\text{rot}} \frac{\partial v(r, \phi)}{\partial \phi} + v(r, \phi) \frac{\partial v(r, \phi)}{\partial r} = 0$$

## Observational data

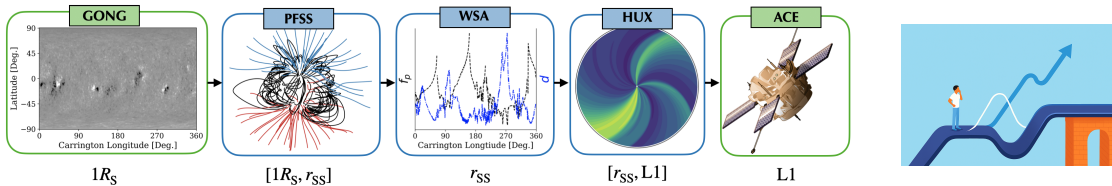
- Global Oscillations Network Group (**GONG**) synoptic magnetograms
- Advanced Composition Explorer (**ACE**) *in-situ* measurements at L1

# WSA model is used at NOAA and UK Met Office today



A snapshot taken from NOAA-SWPC website [www.swpc.noaa.gov](http://www.swpc.noaa.gov) on Sept. 11th, 2025.

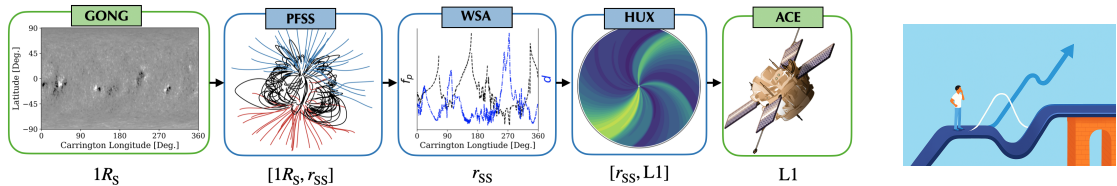
# What are sources of forecast uncertainties?



## ■ Boundary conditions

- ⇒ Different observatories produce different photospheric maps, far-side and polar regions are unobserved, and synoptic magnetograms assume the photosphere is static over 27 days.

# What are sources of forecast uncertainties?



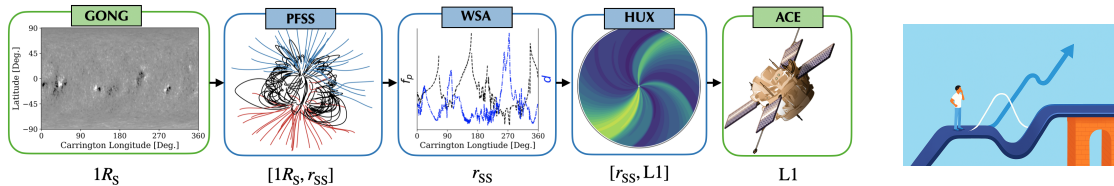
## ■ Boundary conditions

- ⇒ Different observatories produce different photospheric maps, far-side and polar regions are unobserved, and synoptic magnetograms assume the photosphere is static over 27 days.

## ■ Discretization error

- ⇒ Grid resolution can impact forecast accuracy.

# What are sources of forecast uncertainties?



## ■ Boundary conditions

- ⇒ Different observatories produce different photospheric maps, far-side and polar regions are unobserved, and synoptic magnetograms assume the photosphere is static over 27 days.

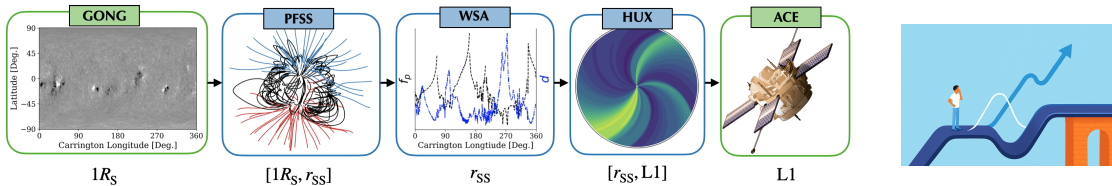
## ■ Discretization error

- ⇒ Grid resolution can impact forecast accuracy.

## ■ Unresolved missing physics

- ⇒ Not resolving kinetic processes which can influence solar wind heating/acceleration.

# What are sources of forecast uncertainties?



## ■ Boundary conditions

- ⇒ Different observatories produce different photospheric maps, far-side and polar regions are unobserved, and synoptic magnetograms assume the photosphere is static over 27 days.

## ■ Discretization error

- ⇒ Grid resolution can impact forecast accuracy.

## ■ Unresolved missing physics

- ⇒ Not resolving kinetic processes which can influence solar wind heating/acceleration.

## ■ Input parameters ⇒ focus of today's talk!

- ⇒ Empirical coefficients and scalars from reduced-physics approximations.

# Model chain parametric uncertainty

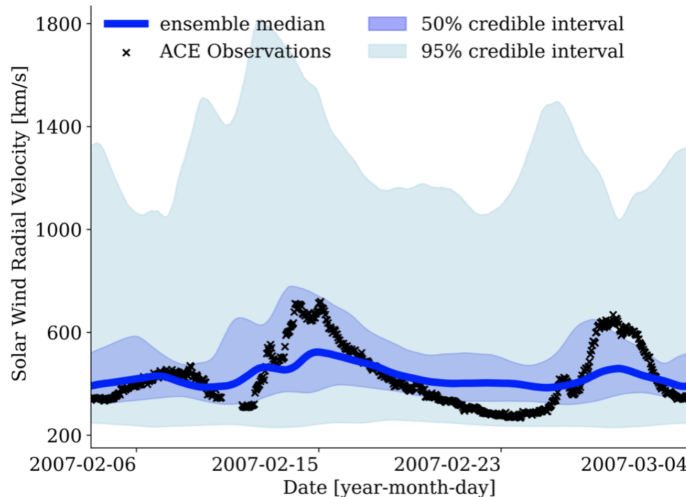
- The model chain has **11 uncertain input parameters** due to reduced physics assumptions and empirical relations.
- Operational forecasts adopt fixed nominal values, which limit **accuracy**.

Parameter	Model	Description	Prior Range
1. $r_{SS}$ [ $R_S$ ]	<b>PFSS</b>	source surface height	[1.5, 4]
2. $v_0$ [ $\frac{\text{km}}{\text{s}}$ ]	<b>WSA</b>	minimum velocity	[200, 400]
3. $v_1$ [ $\frac{\text{km}}{\text{s}}$ ]	<b>WSA</b>	maximum velocity	[550, 950]
4. $\alpha$	<b>WSA</b>	fitting parameter	[0.05, 0.5]
5. $\beta$	<b>WSA</b>	fitting parameter	[1, 1.75]
6. $w$ [rad]	<b>WSA</b>	fitting parameter	[0.01, 0.4]
7. $\gamma$	<b>WSA</b>	fitting parameter	[0.06, 0.9]
8. $\delta$	<b>WSA</b>	fitting parameter	[1, 5]
9. $\psi$	<b>WSA</b>	fitting parameter	[3, 4]
10. $\alpha_{acc}$	<b>HUX</b>	acceleration factor	[0, 0.5]
11. $r_h$ [ $R_S$ ]	<b>HUX</b>	radius acceleration ends	[30, 60]

[Lee et al., 2011, Arden et al., 2014, Meadors et al., 2020, Kumar and Srivastava, 2022, Riley et al., 2015]

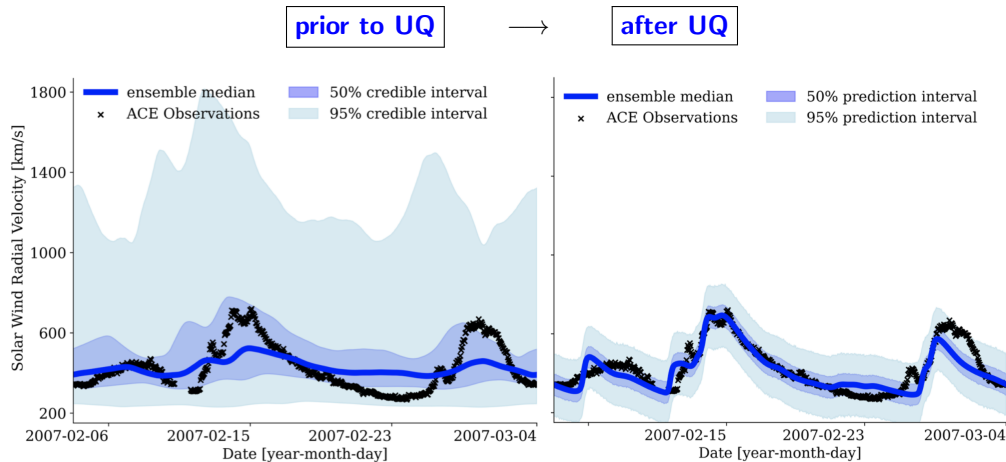
# Parametric uncertainty leads to large forecast uncertainties

Ensembles generated from the prior uniform distributions result in **large credible intervals** and an **inaccurate ensemble median**.

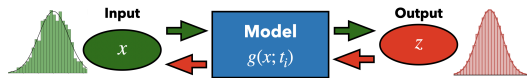


# Fusing information from models and observational data

**"Uncertainty quantification and probabilistic modeling are a key component of providing actionable information to end users"** – 2024 National Academies decadal survey!

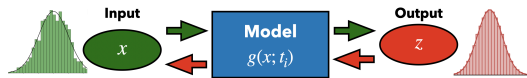


# Uncertainty quantification framework: a step-by-step



Pick model and prepare *in-situ* data  
e.g. PFSS→WSA→HUX and ACE

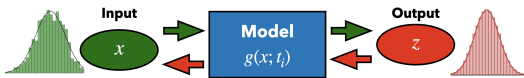
# Uncertainty quantification framework: a step-by-step



Pick model and prepare *in-situ* data  
e.g. PFSS→WSA→HUX and ACE

Identify uncertain parameters  
and define prior assumptions

# Uncertainty quantification framework: a step-by-step

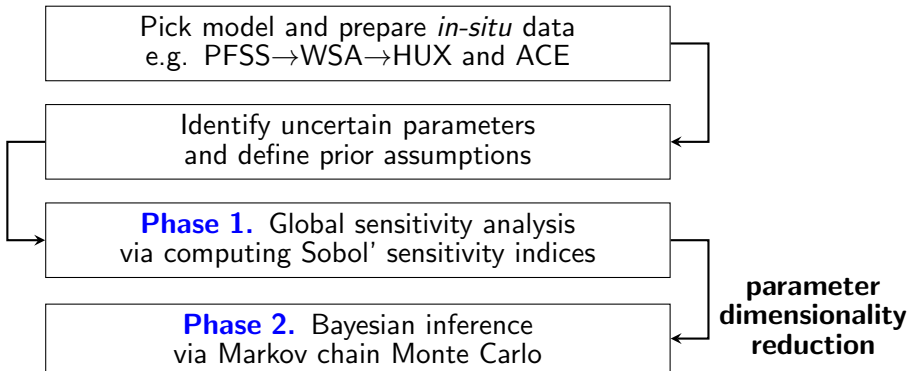
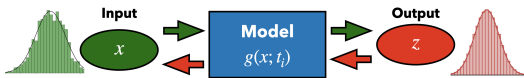


Pick model and prepare *in-situ* data  
e.g. PFSS→WSA→HUX and ACE

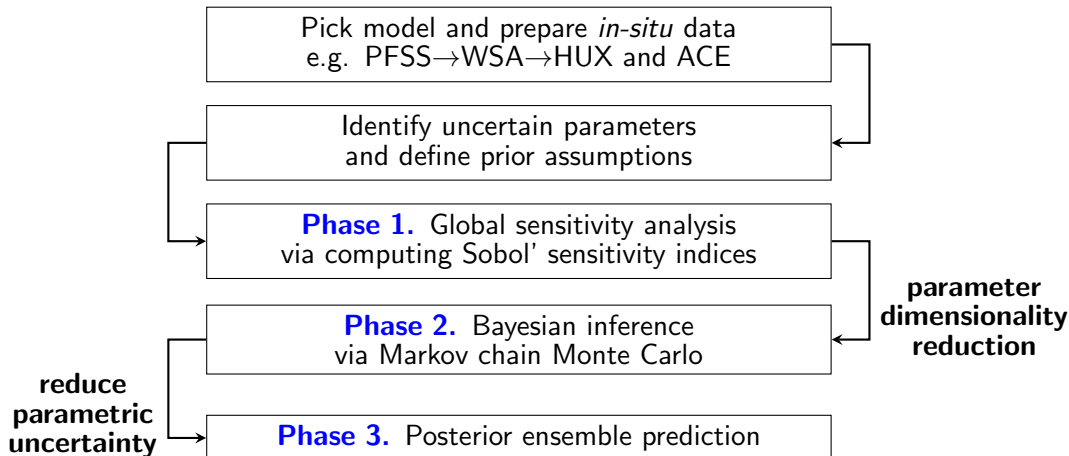
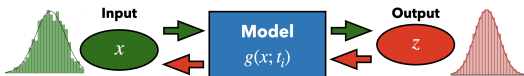
Identify uncertain parameters  
and define prior assumptions

**Phase 1.** Global sensitivity analysis  
via computing Sobol' sensitivity indices

# Uncertainty quantification framework: a step-by-step



# Uncertainty quantification framework: a step-by-step



# Phase 1. Global sensitivity analysis via Sobol' indices

⇒ Identify the most influential parameters based on their contribution to output variance.

## Sobol' sensitivity indices [Sobol', 2001]

$$T_i := \frac{\mathbb{E}_{X \sim i} [\text{Var}_{X_i}(f(X)|X_{\sim i})]}{\text{Var}[f(X)]} = \text{output variance contributed only by } X_i$$

$X := [r_{SS}, v_0, v_1, \alpha, \beta, w, \gamma, \delta, \psi, \alpha_{acc}, r_h]$  uncertain input parameters

$X_i :=$   $i$ th input parameter

$X_{\sim i} :=$  all input parameters excluding the  $i$ th parameter

$f :=$  RMSE between the model radial velocity  
predictions and ACE observations

# Phase 1. Global sensitivity analysis via Sobol' indices

⇒ Identify the most influential parameters based on their contribution to output variance.

## Sobol' sensitivity indices [Sobol', 2001]

$$T_i := \frac{\mathbb{E}_{X \sim i} [\text{Var}_{X_i}(f(X)|X_{\sim i})]}{\text{Var}[f(X)]} = \text{output variance contributed only by } X_i$$

$X := [r_{SS}, v_0, v_1, \alpha, \beta, w, \gamma, \delta, \psi, \alpha_{acc}, r_h]$  uncertain input parameters

$X_i :=$   $i$ th input parameter

$X_{\sim i} :=$  all input parameters excluding the  $i$ th parameter

$f :=$  RMSE between the model radial velocity  
predictions and ACE observations

- **Intuition.** If  $T_i \approx 0$ , then  $\mathbb{E}_{X \sim i} [\text{Var}_{X_i}(f(X)|X_{\sim i})] \approx 0$ , which, by the non-negativity of the variance operator, implies that  $\text{Var}_{X_i}(f(X)|X_{\sim i}) \approx 0$ .

# Phase 1. Global sensitivity analysis via Sobol' indices

⇒ Identify the most influential parameters based on their contribution to output variance.

## Sobol' sensitivity indices [Sobol', 2001]

$$T_i := \frac{\mathbb{E}_{X \sim i} [\text{Var}_{X_i}(f(X)|X_{\sim i})]}{\text{Var}[f(X)]} = \text{output variance contributed only by } X_i$$

$X := [r_{SS}, v_0, v_1, \alpha, \beta, w, \gamma, \delta, \psi, \alpha_{acc}, r_h]$  uncertain input parameters

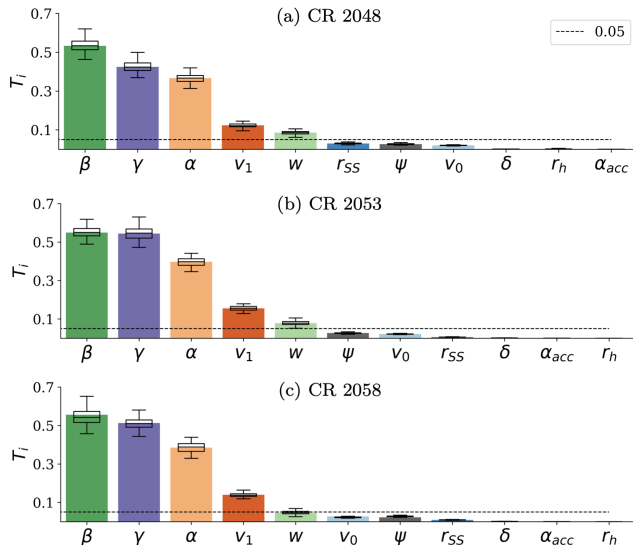
$X_i :=$   $i$ th input parameter

$X_{\sim i} :=$  all input parameters excluding the  $i$ th parameter

$f :=$  RMSE between the model radial velocity  
predictions and ACE observations

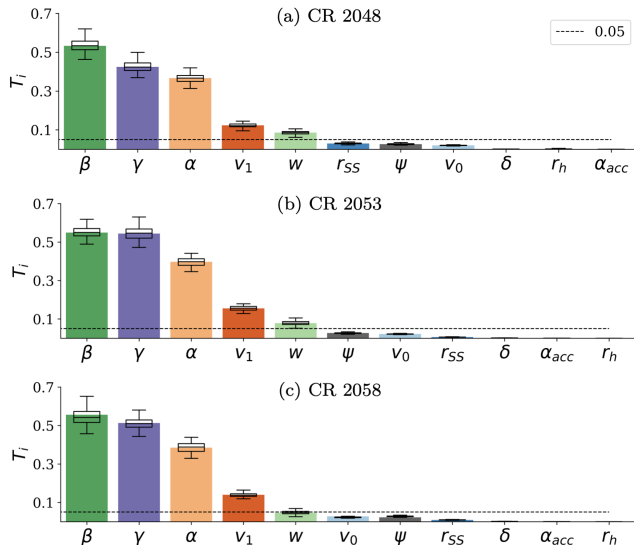
- **Intuition.** If  $T_i \approx 0$ , then  $\mathbb{E}_{X \sim i} [\text{Var}_{X_i}(f(X)|X_{\sim i})] \approx 0$ , which, by the non-negativity of the variance operator, implies that  $\text{Var}_{X_i}(f(X)|X_{\sim i}) \approx 0$ .
- **Estimation.** We estimate  $T_i$  via Monte Carlo estimators, e.g. the Janon and Monod estimator [Janon et al., 2014, Monod et al., 2006].

# Phase 1. Global sensitivity analysis numerical results



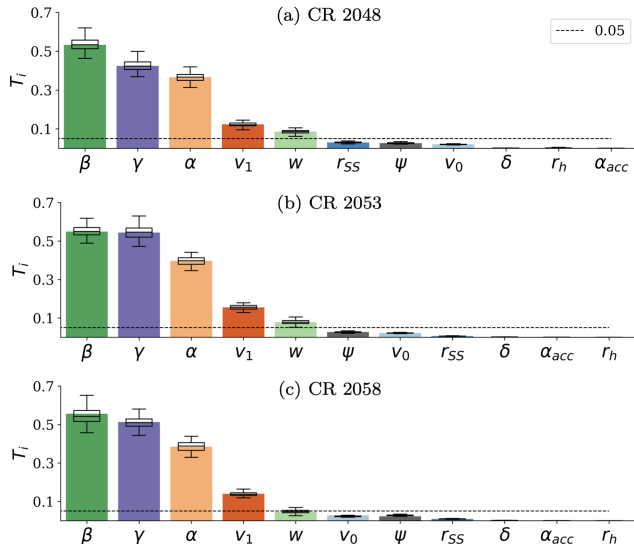
- The five most influential parameters are all from WSA.

# Phase 1. Global sensitivity analysis numerical results



- The **five most influential** parameters are all from **WSA**.
- Meadors et al. (2020) and Majumdar et al. (2025) found that adjusting the **source surface height**  $r_{ss}$  improves the solar wind predictions.

# Phase 1. Global sensitivity analysis numerical results

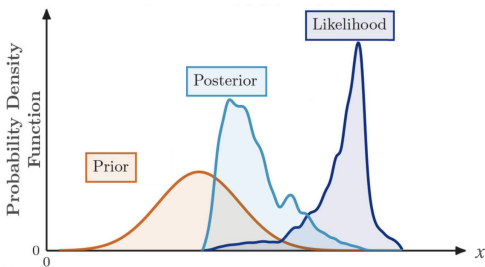


- The **five most influential** parameters are all from **WSA**.
- Meadors et al. (2020) and Majumdar et al. (2025) found that adjusting the **source surface height**  $r_{SS}$  improves the solar wind predictions.
- We found that **in comparison** to all other parameters, it is deemed **non-influential**.

## Phase 2. Bayesian inference

We seek to estimate the **posterior**  $\pi(x|z)$ , which is the probability of the influential parameters  $x$  given ACE measurements at 1-hr cadence  $z = \{z_1, z_2, \dots, z_n\}$ , via **Bayes' rule**:

$$\underbrace{\pi(x|z)}_{\text{Posterior}} \propto \underbrace{\pi(z|x)}_{\text{Likelihood}} \underbrace{\pi(x)}_{\text{Prior}}$$



## Phase 2. Bayesian inference

We seek to estimate the **posterior**  $\pi(x|z)$ , which is the probability of the influential parameters  $x$  given ACE measurements at 1-hr cadence  $z = \{z_1, z_2, \dots, z_n\}$ , via **Bayes' rule**:

$$\underbrace{\pi(x|z)}_{\text{Posterior}} \propto \underbrace{\pi(z|x)}_{\text{Likelihood}} \underbrace{\pi(x)}_{\text{Prior}}$$

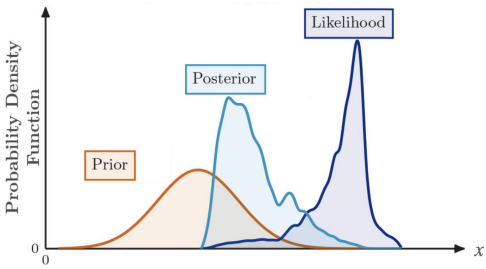
We assume that the model and measurements are related by

$$Z_i = g(X; t_i) + \epsilon_i, \quad i = 1, \dots, n$$

$$\epsilon_i \sim \mathcal{N}(0, \sigma), \quad \sigma = 80 \frac{\text{km}}{\text{s}}$$

resulting in the following likelihood

$$\pi(z|x) \propto \exp \left( -\frac{1}{2\sigma^2} \sum_{i=1}^n [z_i - g(x; t_i)]^2 \right)$$

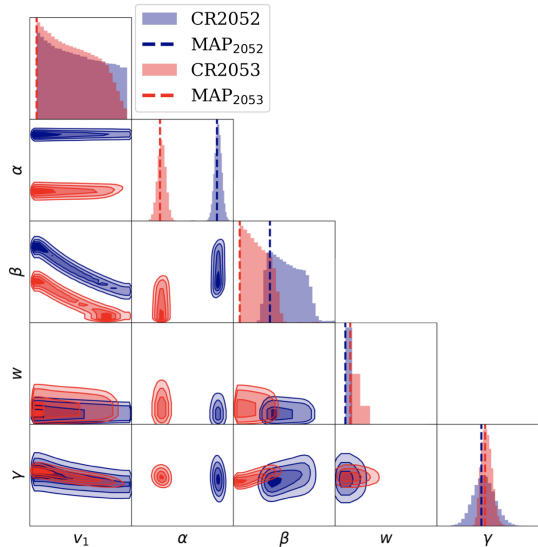


## Phase 2. Bayesian inference numerical results

We use the Markov Chain Monte Carlo (MCMC) Affine Invariant Ensemble Sampler (AIES) [Goodman and Weare, 2010] to generate samples from the posterior density.

AIES main advantages are

1. Affine invariant  $\Rightarrow$  suitable for anisotropic posteriors

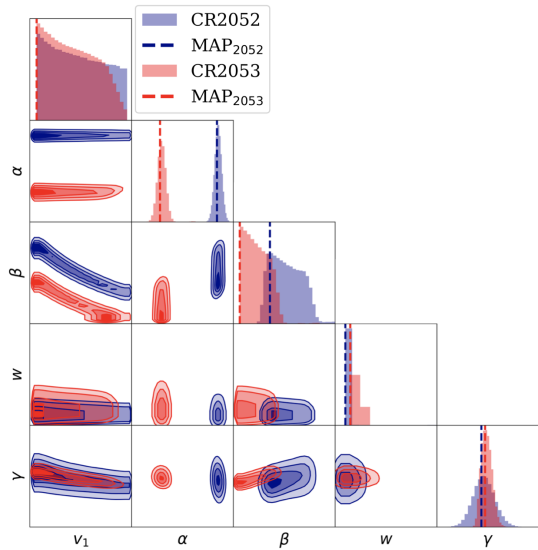


## Phase 2. Bayesian inference numerical results

We use the Markov Chain Monte Carlo (**MCMC**) Affine Invariant Ensemble Sampler (**AIES**) [Goodman and Weare, 2010] to generate samples from the posterior density.

AIES main advantages are

1. Affine invariant  $\Rightarrow$  suitable for anisotropic posteriors
2. Evolves many walkers  $\Rightarrow$  faster convergence

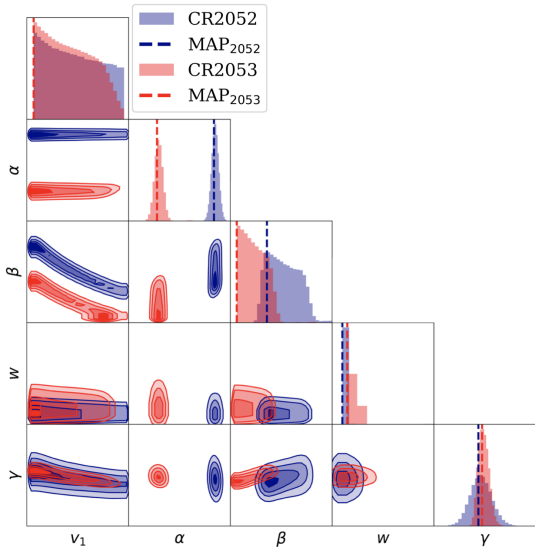


## Phase 2. Bayesian inference numerical results

We use the Markov Chain Monte Carlo (**MCMC**) Affine Invariant Ensemble Sampler (**AIES**) [Goodman and Weare, 2010] to generate samples from the posterior density.

AIES main advantages are

1. Affine invariant  $\Rightarrow$  suitable for anisotropic posteriors
2. Evolves many walkers  $\Rightarrow$  faster convergence
3. *emcee* Python package is well established

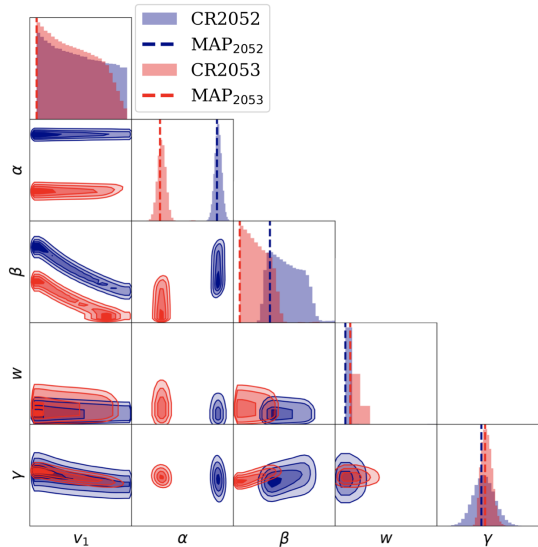


## Phase 2. Bayesian inference numerical results

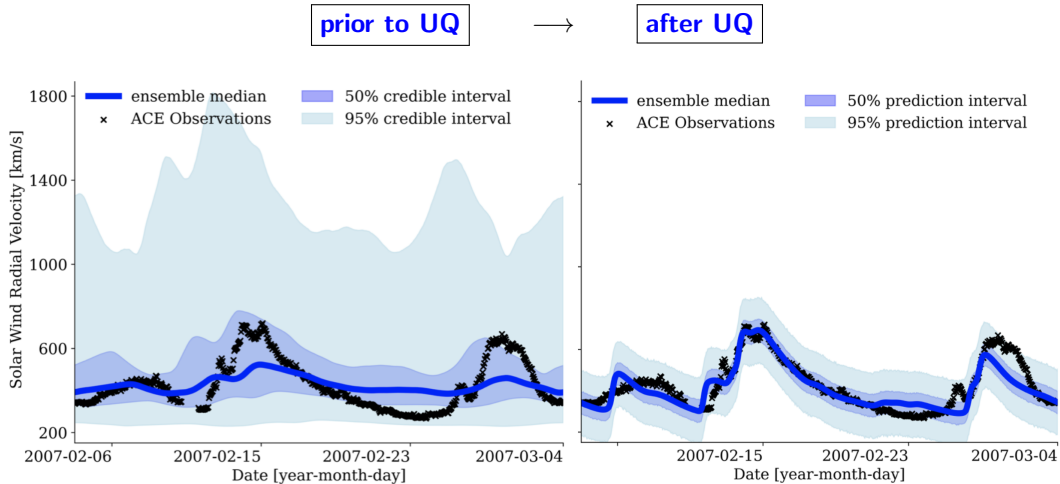
We use the Markov Chain Monte Carlo (**MCMC**) Affine Invariant Ensemble Sampler (**AIES**) [Goodman and Weare, 2010] to generate samples from the posterior density.

AIES main advantages are

1. Affine invariant  $\Rightarrow$  suitable for anisotropic posteriors
2. Evolves many walkers  $\Rightarrow$  faster convergence
3. *emcee* Python package is well established
4. Only two hyperparameters vs.  $d^2$  for standard Metropolis Hastings



## Phase 3. Posterior ensemble predictions

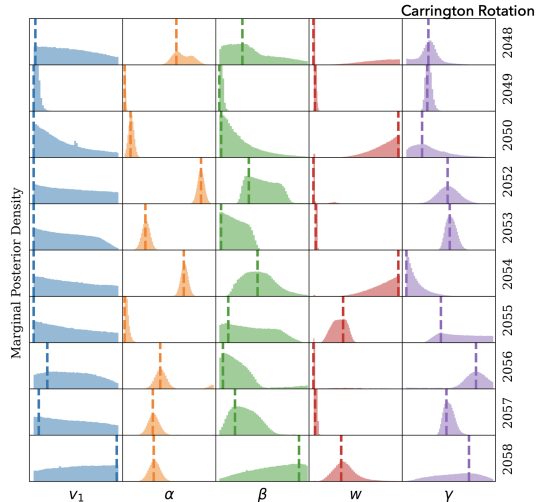


# Can we apply the UQ framework for real-time forecasting?

Ideally, we could use the posteriors from one CR to generate an ensemble for the next.

However, the posterior densities **vary greatly from one CR to the next**.

1. The non-physical parameters are trying to overcompensate the intrinsic and **“hard-wired” limitations** of each of the models.  $\Rightarrow$  Model chain specific...



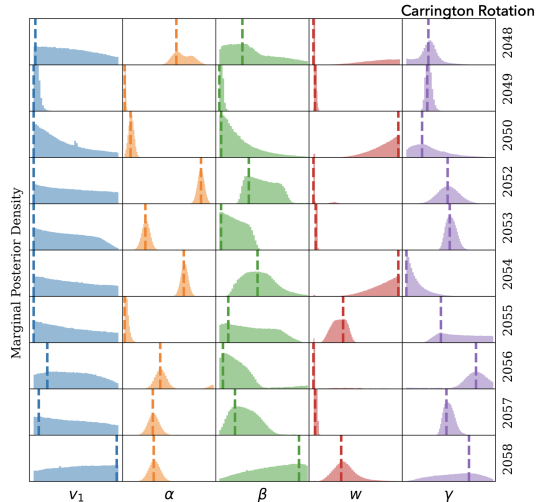
# Can we apply the UQ framework for real-time forecasting?

Ideally, we could use the posteriors from one CR to generate an ensemble for the next.

However, the posterior densities **vary greatly from one CR to the next**.

1. The non-physical parameters are trying to overcompensate the intrinsic and **"hard-wired" limitations** of each of the models.  $\Rightarrow$  Model chain specific...
2. The WSA model is **overparameterized**  $\Rightarrow$  could be **reformulated**

$$v_{\text{wsa}}(f_p, d) = v_0 + \frac{v_1 - v_0}{(1 + f_p)^\alpha} \left( \beta - \gamma \exp \left( - \left( \frac{d}{w} \right)^\delta \right) \right)^\psi$$



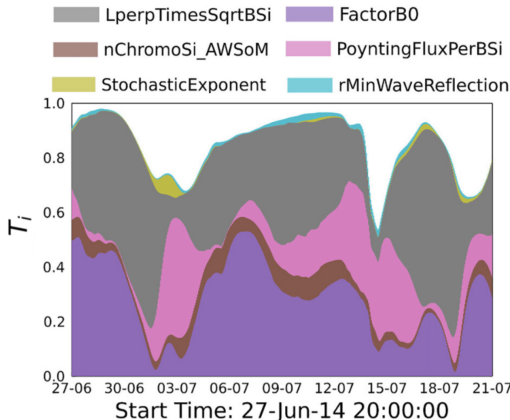
# Computational limitations and alternative methods

The UQ framework requires a large number of model evaluations to reach MC convergence  $1/\sqrt{N}$ .

- $N \approx 10^5$  for the sensitivity analysis (*offline*)
- $N \approx 10^7$  for MCMC (*online*)

Alternative methods for more **computationally expensive model chains** (e.g., WSA-ENLIL):

- Multifidelity unbiased estimators which leverage surrogate models for speeding up MC convergence [Peherstorfer et al., 2018]



Sobol' indices via PCE surrogates for **expensive models** like **AWSOM** [Jivani et al., 2023]

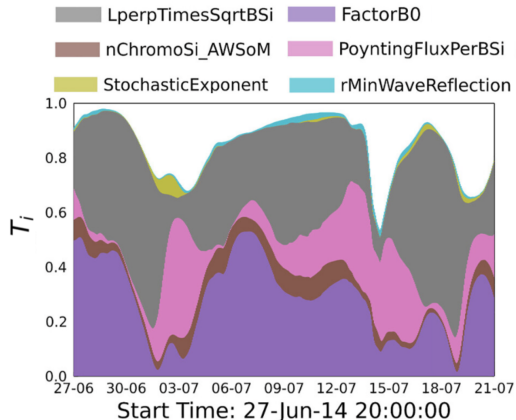
# Computational limitations and alternative methods

The UQ framework requires a large number of model evaluations to reach MC convergence  $1/\sqrt{N}$ .

- $N \approx 10^5$  for the sensitivity analysis (*offline*)
- $N \approx 10^7$  for MCMC (*online*)

Alternative methods for more **computationally expensive model chains** (e.g., WSA-ENLIL):

- Multifidelity unbiased estimators which leverage surrogate models for speeding up MC convergence [Peherstorfer et al., 2018]
- Surrogates include
  1. neural networks
  2. projection-based model reduction via SVD
  3. interpolatory-based, e.g., polynomial chaos expansions (PCEs)

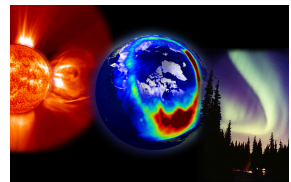


Sobol' indices via PCE surrogates for **expensive models** like **AWSOM** [Jivani et al., 2023]

# UQ study conclusions

- The proposed UQ framework can significantly **reduce** the forecast **uncertainty** and improve median **accuracy**.

*Space Weather* paper link



## Code Accessibility

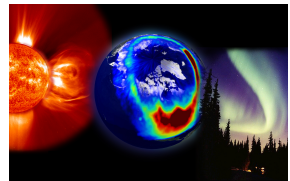
The code used to generate these results is available at [https://github.com/opaliss/Parameter\\_Estimation\\_Solar\\_Wind](https://github.com/opaliss/Parameter_Estimation_Solar_Wind).

Credit: STEREO

# UQ study conclusions

- The proposed UQ framework can significantly **reduce** the forecast **uncertainty** and improve median **accuracy**.
- [Riley et al., 2018] found that the CCMC scoreboard did not show improved CME forecasting capabilities in the **last six years** ⇒ Fusing in-situ data and modeling can potentially show improvements!

*Space Weather* paper link



Credit: STEREO

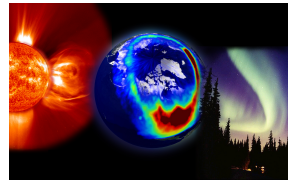
## Code Accessibility

The code used to generate these results is available at [https://github.com/opaliss/Parameter\\_Estimation\\_Solar\\_Wind](https://github.com/opaliss/Parameter_Estimation_Solar_Wind).

# UQ study conclusions

- The proposed UQ framework can significantly **reduce** the forecast **uncertainty** and improve median **accuracy**.
- [Riley et al., 2018] found that the CCMC scoreboard did not show improved CME forecasting capabilities in the **last six years** ⇒ Fusing in-situ data and modeling can potentially show improvements!
- The posterior distributions of the WSA model change greatly over time ⇒ might need reformulation.

*Space Weather* paper link



Credit: STEREO

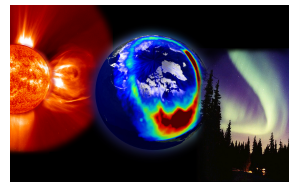
## Code Accessibility

The code used to generate these results is available at [https://github.com/opaliss/Parameter\\_Estimation\\_Solar\\_Wind](https://github.com/opaliss/Parameter_Estimation_Solar_Wind).

# UQ study conclusions

- The proposed UQ framework can significantly **reduce** the forecast **uncertainty** and improve median **accuracy**.
- [Riley et al., 2018] found that the CCMC scoreboard did not show improved CME forecasting capabilities in the **last six years** ⇒ Fusing in-situ data and modeling can potentially show improvements!
- The posterior distributions of the WSA model change greatly over time ⇒ might need reformulation.
- New efforts: WSA+ [Mayank et al., 2025] achieves 40% error reduction using transformers, but there is still room for further progress toward **parsimonious symbolically simplified** WSA.

*Space Weather* paper link



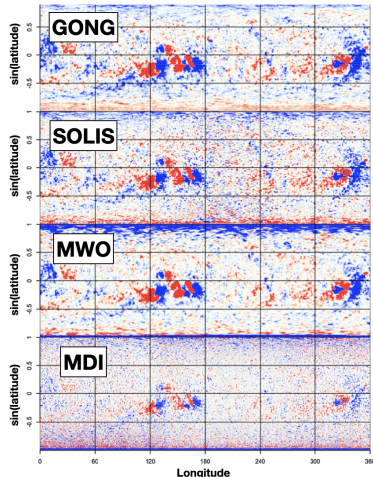
## Code Accessibility

The code used to generate these results is available at [https://github.com/opaliss/Parameter\\_Estimation\\_Solar\\_Wind](https://github.com/opaliss/Parameter_Estimation_Solar_Wind).

Credit: STEREO

# Future directions and outlook

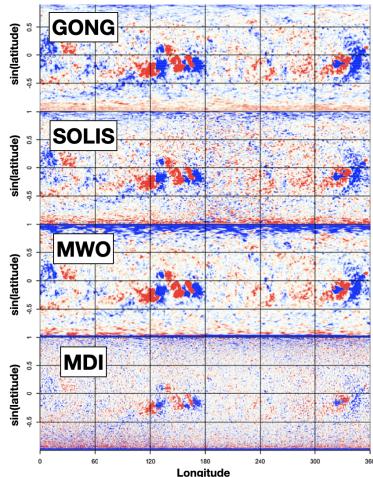
- There are **more sources of uncertainty**, which we need to quantify and reduce:
  1. Considerable differences between magnetograms from **different observatories** [Riley et al., 2014].



Credit: [Riley et al., 2014]

# Future directions and outlook

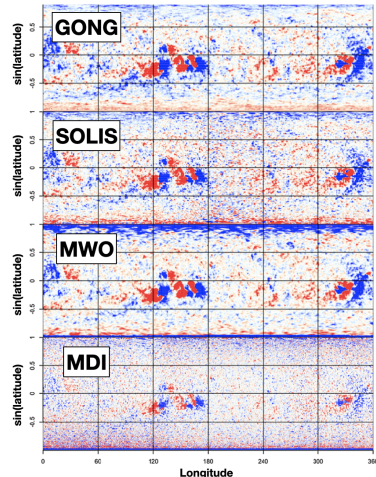
- There are **more sources of uncertainty**, which we need to quantify and reduce:
  1. Considerable differences between magnetograms from **different observatories** [Riley et al., 2014].
  2. **Synoptic magnetograms** far-side and polar regions uncertainties  $\Rightarrow$  leverage **solo** [Downs et al., 2025].



Credit: [Riley et al., 2014]

# Future directions and outlook

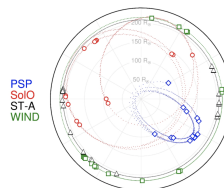
- There are **more sources of uncertainty**, which we need to quantify and reduce:
  1. Considerable differences between magnetograms from **different observatories** [Riley et al., 2014].
  2. **Synoptic magnetograms** far-side and polar regions uncertainties  $\Rightarrow$  leverage **solo** [Downs et al., 2025].
  3. **Grid resolution** can be a source of uncertainty, as pointed out by [Majumdar et al., 2025].



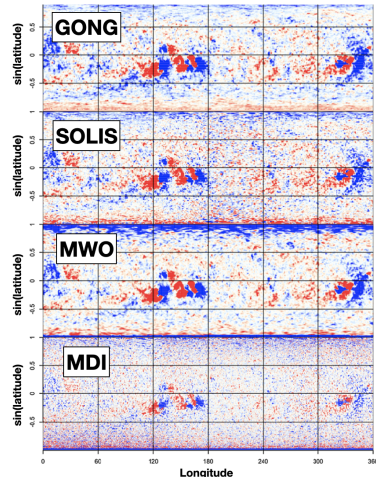
Credit: [Riley et al., 2014]

# Future directions and outlook

- There are **more sources of uncertainty**, which we need to quantify and reduce:
  1. Considerable differences between magnetograms from **different observatories** [Riley et al., 2014].
  2. **Synoptic magnetograms** far-side and polar regions uncertainties  $\Rightarrow$  leverage **soloO** [Downs et al., 2025].
  3. **Grid resolution** can be a source of uncertainty, as pointed out by [Majumdar et al., 2025].



Credit: [Clarkson et al., 2025]



Credit: [Riley et al., 2014]

# Thank you! Questions?



*Solar wind prediction: part physics, part surrealism.*



*Space Weather* paper link

- Altschuler, M. D. and Newkirk, G. (1969).  
Magnetic Fields and the Structure of the Solar Corona. I: Methods of Calculating Coronal Fields.  
*Solar Physics*, 9(1):131–149.
- Arden, W. M., Norton, A. A., and Sun, X. (2014).  
A “breathing” source surface for cycles 23 and 24.  
*Journal of Geophysical Research (Space Physics)*, 119(3):1476–1485.
- Arge, C., Luhmann, J., Odstrcil, D., Schrijver, C., and Li, Y. (2004).  
Stream structure and coronal sources of the solar wind during the may 12th, 1997 cme.  
*Journal of Atmospheric and Solar-Terrestrial Physics*, 66(15):1295–1309.
- Clarkson, D. L., Kontar, E. P., Chrysaphi, N., Emslie, A. G., Jeffrey, N. L., Krupar, V., and Vecchio, A. (2025).  
Tracing the heliospheric magnetic field via anisotropic radio-wave scattering.  
*Scientific Reports*, 15(1):11335.
- Downs, C., Linker, J. A., Caplan, R. M., Mason, E. I., Riley, P., Davidson, R., Reyes, A., Palmerio, E., Lionello, R., Turtle, J., Ben-Nun, M., Stulajter, M. M., Titov, V. S., Török, T., Upton, L. A., Attie, R., Jha, B. K., Arge, C. N., Henney, C. J., Valori, G., Strecker, H., Calchetti, D., Germerott, D., Hirzberger, J., Suárez, D. O., Rodríguez, J. B., Solanki, S. K., Cheng, X., and Wu, S. (2025).  
A near-real-time data-assimilative model of the solar corona.  
*Science*, 388(6753):1306–1310.
- Goodman, J. and Weare, J. (2010).  
Ensemble samplers with affine invariance.  
*Communications in Applied Mathematics and Computational Science*, 5(1):65–80.
- Janon, A., Klein, T., Lagnoux, A., Nodet, M., and Prieur, C. (2014).  
Asymptotic normality and efficiency of two sobol index estimators.  
*ESAIM: Probability and Statistics*, 18:342–364.
- Jivani, A., Sachdeva, N., Huang, Z., Chen, Y., van der Holst, B., Manchester, W., long, D., Chen, H., Zou, S., Huan, X., and Toth, G. (2023).  
Global sensitivity analysis and uncertainty quantification for background solar wind using the alfvén wave solar atmosphere model.  
*Space Weather*, 21(1):e2022SW003262.
- Kumar, S. and Srivastava, N. (2022).  
A parametric study of performance of two solar wind velocity forecasting models during 2006–2011.  
*Space Weather*, 20(9):e2022SW003069.
- Lee, C. O., Luhmann, J. G., Hoeksema, J. T., Sun, X., Arge, C. N., and de Pater, I. (2011).  
Coronal Field Opens at Lower Height During the Solar Cycles 22 and 23 Minimum Periods: IMF Comparison Suggests the Source Surface Should Be Lowered.  
*Solar Physics*, 269(2):367–388.

Majumdar, S., Reiss, M. A., Muglach, K., and Arge, C. N. (2025).  
What causes errors in wang–sheeley–arge solar wind modeling at l1?  
*The Astrophysical Journal*, 988(2):239.

Mayank, P., Camporeale, E., Shrivastav, A. K., Berger, T. E., and Arge, C. N. (2025).  
Neural enhancement of the traditional wang–sheeley–arge solar wind relation.  
*arXiv preprint arXiv:2509.06181*.

Meadors, G. D., Jones, S. I., Hickmann, K. S., Arge, C. N., Godinez-Vasquez, H. C., and Henney, C. J. (2020).  
Data assimilative optimization of wsa source surface and interface radii using particle filtering.  
*Space Weather*, 18(5):e2020SW002464.

Monod, H., Naud, C., and Makowski, D. (2006).  
Uncertainty and sensitivity analysis for crop models.  
*Working with Dynamic Crop Models*, pages 55–100.

Peherstorfer, B., Willcox, K., and Gunzburger, M. (2018).  
Survey of multifidelity methods in uncertainty propagation, inference, and optimization.  
*Siam Review*, 60(3):550–591.

Pizzo, V. (1978).  
A three-dimensional model of corotating streams in the solar wind, 1. theoretical foundations.  
*Journal of Geophysical Research: Space Physics*, 83(A12):5563–5572.

Reiss, M. A., Muglach, K., Mullinix, R., Kuznetsova, M. M., Wiegand, C., Temmer, M., Arge, C. N., Dasso, S., Fung, S. F., González-Avilés, J. J., Gonzi, S., Jian, L., MacNeice, P., Möstl, C., Owens, M., Perri, B., Pinto, R. F., Rastätter, L., Riley, P., and Samara, E. (2022).  
Unifying the validation of ambient solar wind models.  
*Advances in Space Research*.

Riley, P., Ben-Nun, M., Linker, J., Mikic, Z., Svalgaard, L., Harvey, J., Bertello, L., Hoeksema, T., Liu, Y., and Ulrich, R. (2014).  
A multi-observatory inter-comparison of line-of-sight synoptic solar magnetograms.  
*Solar Physics*, 289.

Riley, P., Linker, J. A., and Arge, C. N. (2015).  
On the role played by magnetic expansion factor in the prediction of solar wind speed.  
*Space Weather*, 13(3):154–169.

Riley, P. and Lionello, R. (2011).  
Mapping Solar Wind Streams from the Sun to 1 AU: A Comparison of Techniques.  
*Solar Physics*, 270:575–592.

Riley, P., Mays, M. L., Andries, J., Amerstorfer, T., Biesecker, D., Delouille, V., Dumbović, M., Feng, X., Henley, E., Linker, J. A., Möstl, C., Nuñez, M., Pizzo, V., Temmer, M., Tobiska, W. K., Verbeke, C., West, M. J., and Zhao, X. (2018).

Forecasting the arrival time of coronal mass ejections: Analysis of the ccmc cme scoreboard.

*Space Weather*, 16(9):1245–1260.

Samara, E., Arge, C. N., Pinto, R. F., Magdalenić, J., Wijsen, N., Stevens, M. L., Rodriguez, L., and Poedts, S. (2024).

Calibrating the wsa model in euhforia based on parker solar probe observations.

*The Astrophysical Journal*, 971(1):83.

Sobol', I. (2001).

Global sensitivity indices for nonlinear mathematical models and their monte carlo estimates.

*Mathematics and Computers in Simulation*, 55(1):271–280.

The Second IMACS Seminar on Monte Carlo Methods.

Webb, D. F. and Howard, T. A. (2012).

Coronal mass ejections: Observations.

*Living Reviews in Solar Physics*, 9(1):1–83.